Unsupervised Change Detection on SAR Images using Fuzzy Hidden Markov Chains

Cyril Carincotte, Stéphane Derrode and Salah Bourennane

***Abstract*— This work deals with unsupervised change detection in temporal sets of Synthetic Aperture Radar (SAR) images. We focus on one of the most widely used change detector in the SAR context, the so-called log-ratio. In order to deal with the classification issue, we propose to use a new fuzzy version of Hidden Markov Chains (HMC), and thus to address fuzzy change detection with a statistical approach. The main characteristic of the proposed model is to simultaneously use Dirac and Lebesgue measures at the class chain level. This allows the coexistence of hard pixels (obtained with the classical HMC segmentation) and fuzzy pixels (obtained with the fuzzy measure) in the same image. The quality assessment of the proposed method is achieved with several bi-date sets of simulated images, and comparisons with classical HMC are also provided. Experimental results on real ERS-PRI images confirm the effectiveness of the proposed approach.**

***Index Terms*— SAR images, change detection, log-ratio detector, fuzzy hidden Markov chain, ICE estimation, MPM classification.**

I. Introduction

MULTI-TEMPORAL change detection aims at discerning areas of change on digital images between two or more dates. These change features can be of various type, origin and duration, which allows to distinguish several families of applications, between (1) *land cover monitoring*, which principally consists in detecting the seasonal vegetation changes; (2) *land use monitoring*, which is the characterization of changes mostly due to human activities, like deforestation or urban development; and (3) *damage mapping*, which is the localization of changes caused by natural disasters like earthquake, floods or forest fire, and which are usually supposed to be fast changes. In this work, we are mainly concerned with the third category, in which changes can be detected with an image pair enclosing the event (before / after).

Recent reviews [1], [2] reveal a lack of the use of radar data for thematic application of change detection. Indeed, studies related to satellite-based SAR imagery change detection are much fewer and more recent [3]–[7] than optical-based ones. Nonetheless, SAR sensors hold a strong potential for change detection studies, especially thanks to their all-weather mapping capability, and can also guarantee operational systems in presence of critical atmospheric circumstances and night conditions of illumination. This lack can be explained by the fact that unsupervised change detection on SAR images is made more difficult, mainly for the following reasons:

- the image modality with the presence of speckle inherent to coherent imaging systems/sensors;
- the difference of incidence angle (angle of sight and ascending/descending orbits) of the acquisitions;
- problems related to the difference of generation of radar sensors, which can occur when the two images are separated from several years (spatial resolution, intercalibration, ground segment, final product, ...).

It is clear however that the intrinsic limits of optical sensors, in particular their dependence to weather and illumination conditions, are particularly constraining and not very realistic within an operational framework, especially in *damage mapping* situation. Hence, there is a need for development of change detection methodologies adapted to SAR images.

In the general context of change detection, many techniques have been developed and one can distinguish three kinds of methods [2]:

- the classification of some feature maps, such as image differencing, image ratioing, selective principal component analysis [8] or mutual information [9], into "Change" and "NoChange" classes;
- the comparison of the individual classifications, usually called Post-Classification Comparison (PCC) [10] to identify changed areas;
- the direct and joint classification of the pair of images [7]. Classes where change occurred are expected to present statistics significantly different from where change did not take place [11].

Most of the existing methods for automatic change detection employ crisp models and consequently neglect the fuzzy aspect of the scene behavior. Thus, these methods do not take into account the change detection complexity and may fail to reach a satisfactory reliability level in complex situations, such as in the context of SAR images. To cope with such situations, fuzzy set theory and classical change detection techniques have recently been combined to perform change detection [10], [12], [13], e.g. in spectral-spatial features maps [14], in PCC context [15], as well as in pseudo-joint classification comparison [16].

Indeed, the three kinds of methods previously detailed consider the change detection problem as an image classification issue, of either the feature map, or the pair of original/classification images. To address classification, Hidden Markov Random Fields (HMRF) and HMC models have already proved their efficiency and robustness [17], especially in SAR imagery [18]. Furthermore, HMRF and HMC have also been used in change detection context respectively in [19],

Manuscript received February 01, 2005; revised September 21, 2005.

The authors are with the Department of Multidimensional Signal Processing Group, Institut Fresnel (CNRS-UMR 6133), D.U. de Saint Jérôme, 13397 Marseille Cedex 20 - FRANCE (e-mail: cyril.carincotte@fresnel.fr)

[20] and [7].

In this paper, we address the case of log-ratio feature map classification, based on a new fuzzy HMC model. The log-ratio operator is well-suited to SAR imagery according to the multiplicative nature of speckle. We assume that images have been geometrically corrected and co-registered, and we consequently consider the change detection problem as an unsupervised classification problem of the log-ratio image, with "Change" and "NoChange" classes.

The main contribution of this work is to combine both statistical and fuzzy approaches, in a new fuzzy HMC (f-HMC) model [21], to address the unsupervised change detection task in the SAR context. The paper is organized as follows: first of all, the problem is formulated in Sec. II and the f-HMC model structure is then described in Sec. III. The unknown parameters estimation, achieved with an extension of the Iterative Conditional Estimation (ICE) method [22] is presented in Sec. IV. We also discuss the implementation issues required for the application. Experimental results on simulated data sets are detailed in Sec. V, where quantitative comparisons with classical HMC model are also provided. Sec. VI presents change detection maps obtained on a bi-date set of SAR images showing floods. Conclusions and perspectives are drawn in Sec. VII.

II. Problem formulation

The conventional ratio edge detector [23] is a pixel-by-pixel ratio of mean reflectivity values of the two date images. This detector is well-known and widely used in SAR imagery due to its ability to greatly reduce the speckle influence on the change map. In order to uncompress the range of variation of the image ratio, and to ensure the model adequacy for change detection purpose, we prefer to use the log-ratio detector [24], [25], which is defined as the logarithm of the ratio of average intensities computed on a window of size w, as follows:

$$I_{log-ratio}(i,j) = \log\left(\frac{\sum_{(k,l)\in V_{ij}} I_2(k,l)}{\sum_{(k,l)\in V_{ij}} I_1(k,l)}\right),$$

where V_{ij} defines the neighboring pixels of the pixel (i,j), in a window of size w.

Usually, the change detection task is considered as a 2-class decision process, i.e. the identification of pixels representing "NoChange" (NC) and those representing "Change" (C) from the first image date to the next. Nevertheless, by distinguishing different typologies of changes, the change detection issue can also be considered as a 3-class segmentation problem.

Hence, the histogram of the log-ratio image depicts a range of pixel values from negative to positive numbers, where those clustered around zero represent "NoChange" (NC) and those at either tail represent reflectance changes from one image date to the next. These changes can be divided into two categories; "Negative Changes" ($C-$) and "Positive Changes" ($C+$) (see Fig. 1). The histogram of the log-ratio image can thus be considered as a mixture of three different distributions, and our aim is then to identify these three distributions in order to perform the change detection.

Remark: It worths noting that this model is also available in the classical case in which only one typology of changes is assumed between the two acquisitions. In this case, the 2-class f-HMC model proposed in [21] can directly be applied to the log-ratio image.

In this context, the change detection problem becomes an unsupervised classification problem of the log-ratio image, with three classes $C-$, NC and $C+$. We propose to use a fuzzy version of hidden Markov chain in order to deal with the unsupervised classification issue. Our approach consists in preserving the property and robustness of the classical HMC and enriches it with fuzzy measure characteristics. The distinction between statistical and fuzzy approaches is based on how the information is captured by each concept. In randomness, the information is estimated by an uncertainty measure, while in fuzziness, the information is characterized by an imprecision measure. In fact, fuzzy and probabilistic approaches are complementary rather than competitive. The principle of our model is to exploit the complementarity of fuzzy and probabilistic approaches, combining their pros in a f-HMC model.

In the change detection context, the introduction of the fuzzy measure $\overline{A}$: "the pixel belongs to the class NC", and its associated fuzzy membership functions presented in Fig. 1, will allow us to characterize the imprecision of the log-ratio image.

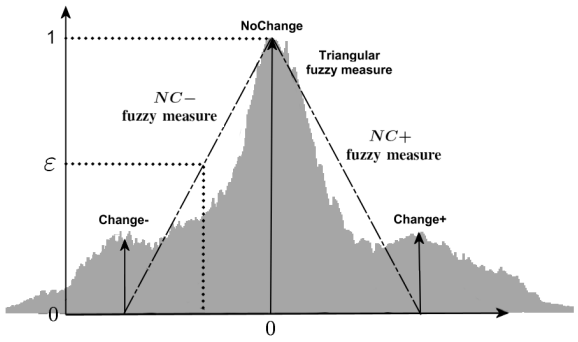

Fig. 1. Fuzzy membership functions $\overline{A}_{NC-}$ and $\overline{A}_{NC+}$ respectively defining the two fuzzy classes $NC-$ and $NC+$, drawn over a log-ratio image histogram.

As shown in Fig. 1, the triangular fuzzy membership function $\overline{A}$ can be decomposed in two linear fuzzy membership functions, $\overline{A}_{NC-}$ and $\overline{A}_{NC+}$ defining respectively the two fuzzy classes $NC-$ and $NC+$. In fact, $NC-$ and $NC+$ correspond respectively to the imprecision measure between $C-$ and NC, and NC and $C+$. $NC-$ and $NC+$ can also respectively be seen as classes corresponding to the mixture of $C-$ and NC, and the mixture of NC and $C+$.

Thus, the principle of the proposed method will be to carry out the fuzzy segmentation of the log-ratio image, by identifying:

- pixels exclusively belonging to classes $C-$, NC or $C+$, which will be qualified as "hard" classes in what follows,
- pixels simultaneously belonging to several hard classes, i.e. belonging to the fuzzy classes $NC-$ (mixture of $C-$

and NC) and $NC+$ (mixture of NC and $C+$).

III. New Fuzzy hidden Markov chains

The success of HMC models is due to the fact that when the unobservable process $\boldsymbol{X}$ can be modeled by a finite Markov chain and when the noise is not too complex, then $\boldsymbol{X}$ can be recovered from the observed process $\boldsymbol{Y}$ using different Bayesian classification techniques like Maximum A Posteriori (MAP), or Maximal Posterior Mode (MPM).

Nevertheless, it is sometimes interesting not to take into account the uncertainty measure of the noisy observation anymore (characteristic of probabilistic approach in classical HMC), but to replace it with an imprecision measure of this observation (characteristic of fuzzy approach) [26]–[28]. However, by adding a fuzzy measure in a statistical model, we obtain an original model, different from both classical and fuzzy models previously cited. Indeed, this introduction has already been achieved in the 2-class case in unsupervised image segmentation for different estimation contexts: blind and contextual [29], HMRF [30]–[32] and very recently in HMC [21].

The way used to introduce the fuzzy measure in these models in the 2-class case was to consider that the Markovian process does not take its values in a discrete 2-uplet anymore, but in a continuous interval. In the change detection context described above, we have to extend this to three classes, i.e. $C-$, NC and $C+$. Indeed, the general K-class case implies the definition of a measure ν on $[0,1]^K$, which is far from being trivial due to memory overflow during computation. In the following, we present an extension of the 2-class f-HMC model proposed in [21] to the 3-class case, and its application to change detection. Since the intensities of the two fuzzy classes ($NC-$ and $NC+$) do not overlap and each fuzzy class is mixed of only two hard classes, the 2-class f-HMC described in [21] can be directly applied to each fuzzy class $NC-$ and $NC+$.

A. Fuzzy HMC modelization

In the unsupervised image segmentation based on HMC theory, the 2D image needs to be converted in a 1D sequence, thanks to the use of a Hilbert-Peano scan on the image [33] (see Fig 2).

The Hilbert-Peano scan belongs to the family of Space Filling Curves (SFCs), which include the Z-order, the zig-zag and the standard raster scans. SFCs have been used in a wide variety of image processing applications such as compression, half-toning, pattern recognition and texture analysis (see [34], [35] and references cited therein). All these scans can be used to convert a 2D set of pixels into a 1D sequence. Nevertheless, the Hilbert-Peano scan furnishes a good exploitation of the 2D locality. This property, together with the pseudo randomness of direction changes in the scan, implies that the Hilbert-Peano scan would work well (statistically) for a large family of images, especially for real images.

So, let consider two sequences of random variables $\boldsymbol{X} = \{X_1, \ldots, X_N\}$ and $\boldsymbol{Y} = \{Y_1, \ldots, Y_N\}$ corresponding respectively to the desired change detection map and the log-ratio image that has to be segmented, according to the Hilbert-Peano scan.

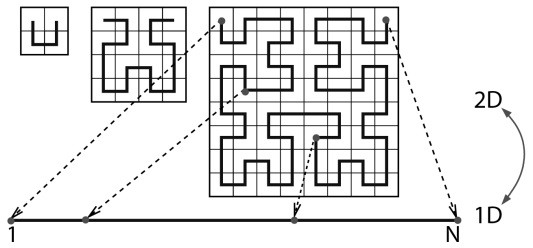

Fig. 2. Construction of a Hilbert-Peano scan for a 8×8 image (initialisation, intermediate stage and result) (N = number of pixels in the image).

For the sake of comprehension, -1, 0 and 1 will respectively denote the hard classes $C-$, NC and $C+$. In a 3-class HMC approach, each X_n takes its value in the finite set of classes $\psi = \{-1, 0, 1\}$ and each Y_n takes its value in the set of real numbers $\mathbb{R}$. In the f-HMC context, the range of X_n is now the interval $\Psi = [-1, 1]$. In the following, $\boldsymbol{\varepsilon_n}$ will denote a realization of random variables X_n and we will adopt the notation:

- $\varepsilon_n = -1$ if the pixel is from class $C-$,
- $\varepsilon_n \in]-1, 0[$ if the pixel is a fuzzy one belonging to $NC-$,
- $\varepsilon_n = 0$ if the pixel is from class NC.
- $\varepsilon_n \in]0, 1[$ if the pixel is a fuzzy one belonging to $NC+$,
- $\varepsilon_n = 1$ if the pixel is from class $C+$.

B. Probabilities in fuzzy HMC context

In the 3-class case, the HMC approach requires the definition of *a priori* and state transition probabilities on ψ. Similarly, we now have to define these probabilities on Ψ.

As stated previously, each X_n contains two types of components: three hard ones $(-1, 0, 1)$ and two fuzzy ones $(]-1, 0[,]0, 1[)$. Let δ_{-1}, δ_0 and δ_1 be Dirac weights on -1, 0 and 1, and υ_{-1} and υ_1 the Lebesgue measures on $]-1, 0[$ and $]0, 1[$. By taking $\nu = \delta_{-1} + \delta_0 + \delta_1 + \upsilon_{-1} + \upsilon_1$ as a measure on Ψ, the distribution of X_n can be defined by a density h on Ψ with respect to ν.

If we assume that $\boldsymbol{X}$ is homogeneous and the distribution of each X_n is uniform on the fuzzy class, $h(\varepsilon_n) = P(X_n = \varepsilon_n) = \pi_{\varepsilon_n}$ can be written:

$$\begin{aligned} h(\varepsilon_n = -1) &= \pi_{-1}, \\ h(\varepsilon_n = 0) &= \pi_0, \\ h(\varepsilon_n = 1) &= \pi_1, \\ h(\varepsilon_n) &= \pi_{NC-}, \forall \varepsilon_n \in]-1, 0[, \\ h(\varepsilon_n) &= \pi_{NC+}, \forall \varepsilon_n \in]0, 1[, \end{aligned}$$

with $\pi_{-1} + \pi_0 + \pi_1 + \pi_{NC-} + \pi_{NC+} = 1$.

We can now detail the new expression for the transition

probabilities of the Markov chain:

$$\begin{aligned} &P\left(X_n=\varepsilon_n \mid X_{n-1}=\varepsilon_{n-1}\right)= \\ &P\left(X_n=-1 \mid X_{n-1}=\varepsilon_{n-1}\right)\delta_{-1}(\varepsilon_n) \\ &+P\left(X_n=\varepsilon_n \mid X_{n-1}=\varepsilon_{n-1}\right)1_{]-1,0[}(\varepsilon_n) \\ &+P\left(X_n=0 \mid X_{n-1}=\varepsilon_{n-1}\right)\delta_{0}(\varepsilon_n) \\ &+P\left(X_n=\varepsilon_n \mid X_{n-1}=\varepsilon_{n-1}\right)1_{]0,1[}(\varepsilon_n) \\ &+P\left(X_n=1 \mid X_{n-1}=\varepsilon_{n-1}\right)\delta_{1}(\varepsilon_n). \end{aligned}$$

This leads to the matrix of state transition probabilities $\boldsymbol{T}=\left\{t_{\varepsilon_{n-1},\varepsilon_n}\right\}$ defined by:

$$t_{\varepsilon_{n-1},\varepsilon_n}=P\left(X_n=\varepsilon_n \mid X_{n-1}=\varepsilon_{n-1}\right),$$

$\forall\ \varepsilon_{n-1},\varepsilon_n\in\Omega$ and $\forall\ n\in\{2,\ldots,N\}$, with the entries having the properties:

$$t_{\varepsilon_{n-1},\varepsilon_n}\geq 0 \quad \text{and} \quad \sum_{\varepsilon_{n-1}\in\Omega} t_{\varepsilon_{n-1},\varepsilon_n}=1.$$

C. Fuzzy HMC implementation

Similarly to HMC, f-HMC based image segmentation methods consider the two following assumptions:

- the random variables $Y_1,\ldots,Y_N$ are independent conditionally on $\boldsymbol{X}$;
- the distribution of each Y_n conditionally on $\boldsymbol{X}$ is equal to its distribution conditionally on X_n.

Furthermore and similarly to HMC, we get:

$$P\left(\boldsymbol{X}=\boldsymbol{x}\right)=\pi_{\varepsilon_1}\prod_{n=2}^{N} t_{\varepsilon_{n-1},\varepsilon_n}.$$

Assuming that distributions of $(X_n,Y_n,X_{n+1},Y_{n+1})$ are independent of n, each state ε_n of the state space (i.e. hard classes $-1,0,1$, as well as fuzzy classes]-1,0[and]0,1[) is associated to a distribution characterizing the pixel intensities of the corresponding class:

$$f_{\varepsilon_n}(y_n)=P\left(Y_n=y_n \mid X_n=\varepsilon_n\right). \tag{1}$$

Given an observed sequence $\boldsymbol{y}=\{y_1,\ldots,y_N\}$ (in our case the log-ratio image via the Hilbert-Peano scan), the joint state-observation probability is given by:

$$P\left(\boldsymbol{X}=\boldsymbol{x},\boldsymbol{Y}=\boldsymbol{y}\right)=\pi_{\varepsilon_1}\ f_{\varepsilon_1}(y_1)\prod_{n=2}^{N} t_{\varepsilon_{n-1},\varepsilon_n} f_{\varepsilon_n}(y_n).$$

In unsupervised classification, the distribution $P\left(\boldsymbol{X}=\boldsymbol{x},\boldsymbol{Y}=\boldsymbol{y}\right)$ is unknown and must first be estimated in order to apply a Bayesian classification technique. Therefore the following sets of parameters need to be estimated:

1) The set $\boldsymbol{\Gamma}$ characterizing the Markov chain parameters, i.e. the initial probability vector $\boldsymbol{\pi}=(\pi_\varepsilon)_{\forall\varepsilon\in\Omega}$ and the transition probability matrix $\boldsymbol{T}$.
2) The set $\boldsymbol{\Delta}$ regrouping the parameters of the probability density functions in Eq. (1). In the Gaussian case, $\boldsymbol{\Delta}$ is composed of means and variances.

Note: In the following, we only consider Gaussian distributions, but this is not a restriction of the model. Indeed, the model can be used for generalized, i.e. non-Gaussian, mixture estimation, with parametric as well as non parametric densities estimation techniques.

IV. Parameters estimation with ICE

For the estimation of the parameters in $\boldsymbol{\Theta}=\{\boldsymbol{\Gamma},\boldsymbol{\Delta}\}$, we propose to use an adaptation of the general ICE algorithm [22], [29] which can be seen as an alternative to the well-known Estimation-Maximization (EM) algorithm. This section is not intended to give a complete description of the ICE algorithm in the HMC context, interested readers may consult [18], [36].

A. ICE principle

In fact, ICE does not refer to the likelihood, a notion which is difficult to handle in the context of our study, but it is based on the conditional expectation of some estimators from the complete data $(\boldsymbol{x},\boldsymbol{y})$. It is an iterative method which produces a sequence of estimations θ^q of parameter θ as follows:

1) initialization θ^0, obtained with an initial segmentation algorithm (k-means algorithm).
2) computation of $\theta^{q+1}=E_q[\hat{\theta}(\boldsymbol{X},\boldsymbol{Y})\ \Big|\ \boldsymbol{Y}=\boldsymbol{y}]$, where $\hat{\theta}(\boldsymbol{X},\boldsymbol{Y})$ is an estimator of θ.
3) stop the algorithm when $\theta^{Q-1}\approx\theta^{Q}$.

This procedure leads to two different situations detailed in next sub-sections.

B. Estimation of parameters in $\boldsymbol{\Gamma}$

Similarly to the classical case, parameters in $\boldsymbol{\Gamma}$ can be calculated analytically by using the Baum-Welch algorithm:

- for the hard classes, the classical normalized Baum-Welch probabilities can be used directly.
- for the fuzzy classes, the forward and backward probabilities have to be defined for each fuzzy class.

For the fuzzy class $NC-$, the forward and backward probabilities are defined by:

$$\begin{aligned} \alpha_{n+1}(\xi) &\propto \int_{-1}^{0} \alpha_n(\zeta)\ t_{\zeta,\xi}\ f_\xi(y_{n+1})\ d\zeta, \\ \beta_n(\xi) &\propto \int_{-1}^{0} \beta_{n+1}(\zeta)\ t_{\xi,\zeta}\ f_\zeta(y_{n+1})\ d\zeta. \end{aligned} \tag{2}$$

For the fuzzy class $NC+$, the forward and backward probabilities are defined by:

$$\begin{aligned} \alpha_{n+1}(\xi) &\propto \int_{0}^{1} \alpha_n(\zeta)\ t_{\zeta,\xi}\ f_\xi(y_{n+1})\ d\zeta, \\ \beta_n(\xi) &\propto \int_{0}^{1} \beta_{n+1}(\zeta)\ t_{\xi,\zeta}\ f_\zeta(y_{n+1})\ d\zeta. \end{aligned} \tag{3}$$

The integrals above can not be solved analytically. A numerical integration must be performed and intervals $]-1,0[$ and $]0,1[$ are partitioned into a given number of sub-intervals.

We though obtain F "discrete fuzzy" classes by interval, whose fuzzy membership degree corresponds to the medium value of the considered sub-interval. The bigger F is, the closer it is from Eq. (2) and Eq. (3), but to the cost of an increase in the computation time.

C. Estimation of parameters in $\mathbf{\Delta}$

Denoting by $\mathcal{N}(m, \sigma^2)$ the normal distribution with mean m and variance σ^2, the pdf of the hard classes can then be expressed by:

$$\begin{aligned} \varepsilon_n = -1 &: \mathcal{N}(m_{-1}, \sigma_{-1}^2), \\ \varepsilon_n = 0 &: \mathcal{N}(m_0, \sigma_0^2), \\ \varepsilon_n = 1 &: \mathcal{N}(m_1, \sigma_1^2). \end{aligned}$$

For the parameters $\mathbf{\Delta}= \{m_{-1}, m_0, m_1, \sigma_{-1}, \sigma_0, \sigma_1\}$, which are in fact the hard classes parameters, θ^{q+1} is not tractable. They can however be estimated by computing the empirical mean of several estimates according to $\theta^{q+1} = \frac{1}{L}\sum_{l=1}^{L} \hat{\theta}(\boldsymbol{x}^l, \boldsymbol{y})$, where $\boldsymbol{x}^l$ is an *a posteriori* realization of $\boldsymbol{X}$ conditionally on $\boldsymbol{Y}$. It can be shown that $\boldsymbol{X} \mid \boldsymbol{Y}$ is a non homogeneous Markov chain whose parameters can be computed with the forward and backward probabilities in Eq. (2) and Eq. (3).

The definition of the fuzzy measure $\overline{A}$: "the pixel belongs to class NC", and its fuzzy membership function μ_A, allows to estimate the fuzzy parameters of the set $\mathbf{\Delta}$ in this new context.

Let define the proposed fuzzy membership function μ_A:

$$\mu_A(m) = \begin{cases} 1 - \frac{m_0 - m}{m_0 - m_{-1}} & \forall m \in [m_{-1}, m_0], \\ 1 - \frac{m_0 - m}{m_0 - m_1} & \forall m \in [m_0, m_1], \\ 0 & \text{elsewhere.} \end{cases} \quad (4)$$

Accordingly, the parameters of the pdf for the fuzzy classes can then be estimated by:

$$\begin{aligned} \varepsilon_n \in]-1, 0[&: \mathcal{N}\left((1-\varepsilon_n)m_{-1} + \varepsilon_n m_0, (1-\varepsilon_n)^2\sigma_{-1}^2 + \varepsilon_n^2\sigma_0^2\right), \\ \varepsilon_n \in]0, 1[&: \mathcal{N}\left((1-\varepsilon_n)m_0 + \varepsilon_n m_1, (1-\varepsilon_n)^2\sigma_0^2 + \varepsilon_n^2\sigma_1^2\right). \end{aligned} \quad (5)$$

Note: In a non-Gaussian context, moments of higher order can be estimated by the extension of Eq. (5) to the considered order, and generalized mixture estimation can thus be achieved.

The estimation of all the parameters in $\mathbf{\Theta}$ allows to implement this new f-HMC model in an unsupervised way. The next section presents the application of this model to unsupervised fuzzy change detection on SAR images.

V. Change detection on noisy simulated images

In practice, extensive data surveys at the time of data acquisitions are rarely achieved. Regarding the real data set used in Sec. VI, ground truth was not available. Indeed, the nature of changes that have to be detected (floods) can make the ground truth establishment very difficult to perform: floods evolve rapidly, soil humidity is quite difficult to quantify, ... So, we perform experiments to assess the change detection accuracy on synthetic data sets, composed of noisy simulated images corrupted by speckle.

A. Simulated data set

The simulation procedure was inspired by radar image formation phenomena: SAR imagery produces data by coherent summation of elementary scattered electromagnetic fields $A\, e^{j\phi}$. If we consider heterogeneous ground areas, each pixel can be simulated by coherent summation of hundreds of reflectivity amplitude A_n and phases ϕ_n. A_n comes from independent realizations of a Gamma distribution defined by a mean reflectivity value μ and an heterogeneous coefficient λ, whereas ϕ_n comes from independent uniform realizations in $[0, 2\pi]$. Taking the square of the modulus of each pixel yields a one-look intensity image.

A two-class Gibbs field (256×256) serves as reference image (Fig. 3-(a)). The corresponding three-look noisy image $t1$ (see Fig. 4-(a)) is then generated according to the procedure described above with ($\mu_1 = 100, \lambda_1 = 15$) and ($\mu_2 = 180, \lambda_2 = 25$), by averaging three independent realizations of speckle.

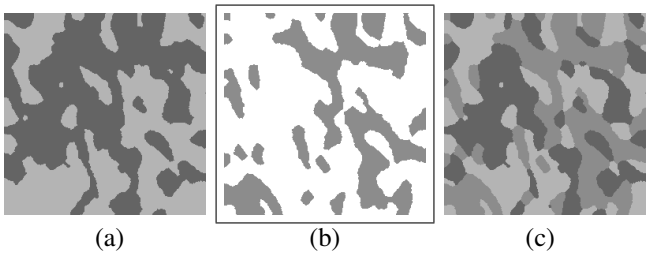

(a) (b) (c)

Fig. 3. (a) Reference image, (b) Ground truth image of simulated changes, and (c) Blurred reflectivity image.

To obtain the $t2$ image, simulated changes areas (Fig. 3-(b)) are inserted in the reference image. The corresponding three-look noisy image $t2$ is then generated according to the procedure described above with $A_C = 140$ and $\lambda_C = 20$ (see Fig. 4-(b)).

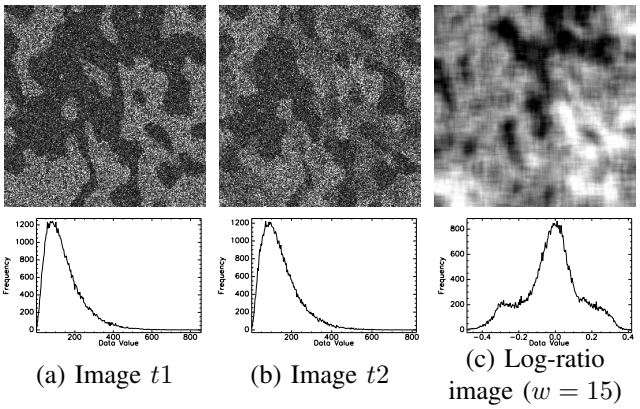

(a) Image $t1$ (b) Image $t2$ (c) Log-ratio image ($w = 15$)

Fig. 4. Simulated data set used in experiments and corresponding histograms. (a) Noisy simulated image $t1$ corresponding to Fig. 3-(a), (b) Noisy simulated image $t2$ obtained by inserting simulated changes in (a), corresponding to Fig. 3-(c), and (c) corresponding log-ratio image ($w = 15$).

B. Experimental protocol

HMC and f-HMC models have been comparatively assessed on the log-ratio image presented in Fig. 4-(c) ($w = 15$). In order to make a valuable comparison, the HMC model used is a 3-class algorithm, corresponding to $C-$, NC and $C+$.

Actually, in all cases, parameters initialization was achieved thanks to the classification obtained with a k-means classifier (estimation from complete data). The ICE algorithm was stopped at iteration Q when $\frac{\|\theta^{Q-1}-\theta^{Q}\|}{\|\theta^{Q-1}\|}$ reaches a given threshold value. The image classification was performed with respect to the fuzzy MPM criterion [31] for the f-HMC model, and with respect to the classical MPM criterion for the HMC model.

The choice of the partitioning of the intervals $]-1,0[$ and $]0,1[$ implies different possible numbers of "discrete" fuzzy classes F, and so different values of the fuzzy measure ε. For example, in the $NC+$ case, $F = 2$ yields $\varepsilon \in \{0.25, 0.75\}$, $F = 3$ yields $\varepsilon \in \{0.166, 0.5, 0.833\}, \ldots$ To make comparison between maps obtained with HMC and f-HMC, a defuzzification has to be performed on the f-HMC ones. Since the values of fuzzy measure ε correspond to the membership degrees of each hard class ("Change" and "NoChange"), a solution is to perform a hard threshold at $\varepsilon = 0.5$. Note that this threshold value has experimentally yielded the best error rates in the following experiments. Finally, we limit the study to $F = 2$ fuzzy classes.

C. Change detection results

Change detection results in terms of hits rate, false alarms rate, and overall rate are presented in Fig. 5. These results have been obtained with HMC, and new f-HMC model ($F = 2$) for various values of the window detector size w. In both models, Gaussian densities have been assumed to model the pixel intensities in the log-ratio image.

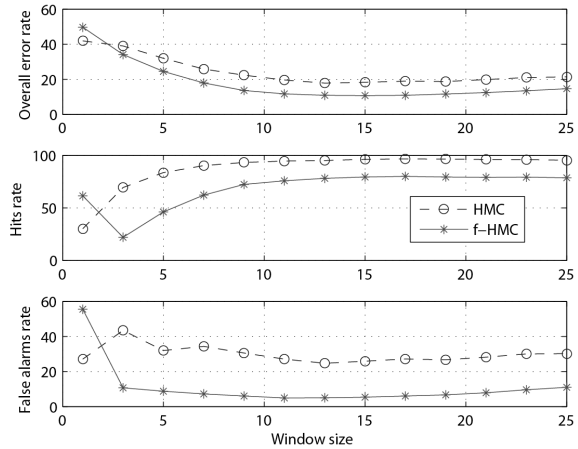

Fig. 5. Change detection results provided by HMC and f-HMC models under Gaussian distributions assumption.

One can see that best results in terms of global error rate are provided by the f-HMC model whatever the window size w. This point clearly highlights the interest of the proposed approach in the SAR context. We can observe that even if the HMC model reaches best hits rate compared to f-HMC, f-HMC significantly reduces the false alarms rate. These comments are confirmed by Fig. 6, which shows the Receiver Operating Characteristic (ROC) curves according to the window detector size w. These curves also confirm that the best window detector size w seems to be around $w = 15$. Finally, the false alarms rate also seems to be less sensitive to the window size for f-HMC model, which allows to significantly reduce the overall error rate.

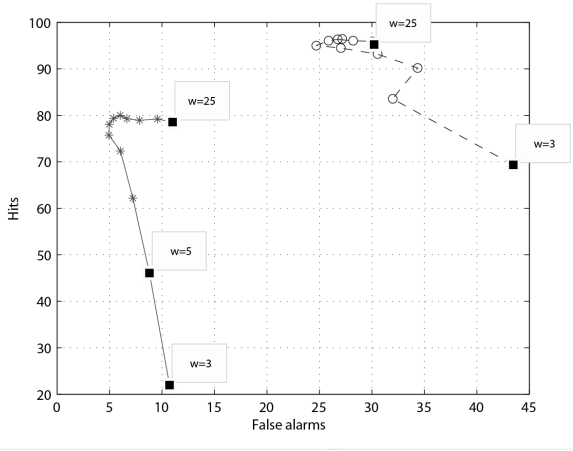

Fig. 6. ROC curves obtained with HMC and f-HMC models under Gaussian distributions assumption according to the window detector size w.

Fig. 7 shows the best change detection maps obtained with HMC ($w = 13$) and f-HMC ($w = 15$) models, and corresponding overall error rates, which is approximatively twice bigger with HMC model. The visual interpretation of the change detection maps, as well as corresponding error rates, show the interest and the precision of the proposed method, even with significant noise.

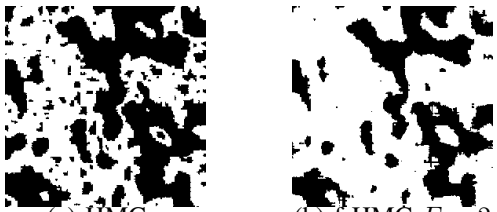

(a) HMC - $w = 13$ 17.84%

(b) f-HMC $F = 2$ - $w = 15$ 10.68%

Fig. 7. Best change detection maps obtained with HMC and f-HMC models.

Fig. 8 presents the distributions obtained through the mixture estimation with f-HMC model ($w = 15$).

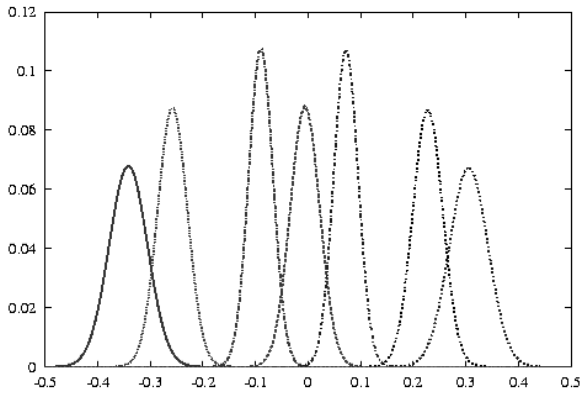

Fig. 8. Pdf arising in mixture estimation obtained with f-HMC model ($F = 2$ - $w = 15$).

The conclusions from this study have been confirmed by other experiments:

- Similar results have been observed for synthetic images of various reflectivity value areas, e.g. $A_1 = 100, A_2 = 140$ and $A_C = 120$, which confirms the robustness of the f-HMC model to reflectivity variation of changed areas.
- In all experiments, the results indicate that the log-ratio detector fits the f-HMC model better than the classical ratio one. This can be explained by the fact that the ratio detector provides a compact (small range) and non-symmetrical histogram, in which positive and negative changes are hard to identify, whereas log-ratio detector yields quite symmetrical histogram, which naturally fits the proposed approach.

VI. Change detection on ERS-PRI data set

Fig. 9 presents bi-date images used to assess the proposed approach in real context. The data are 3-look ERS-2 PRI images with pixel sizes of $12.5m$ in both azimuth and range directions, and are also geo-referenced and co-registered. These images have been acquired on September 9, 2000, and October 21, 2000, around the town of Gloucester (England). The scene corresponds to agricultural regions before and during a flood. Flooded areas, which appear dark due to the specular reflectivity of water, are visible along the river in the middle upper part of Fig. 9-(b).

In addition to the classical SAR images difficulties, several water surfaces of the scene were exposed to the wind, whereas others were sheltered from it. Frictional stress at the interface between the water and the wind causes the water to move in the direction of the wind, which produces changes of different signs in the log-ratio image. Our approach thus seems well-suited to this context.

Fig. 10 presents the log-ratio image ($w = 15$). Indeed, one can distinguish the main areas corresponding to the flood, as well as some unexpected areas where strong changes seem to have occurred.

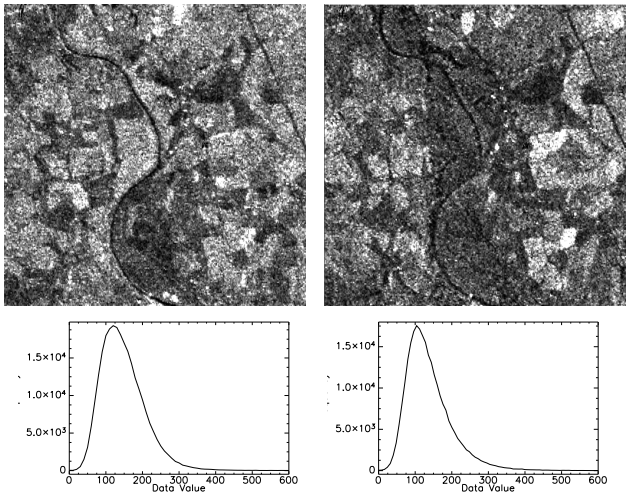

(a) Sept. 09, 2000. (b) Oct. 21, 2000.

Fig. 9. Two co-registered ERS-2 PRI images of agricultural regions near Gloucester, England (512×512) and their corresponding histograms, © ESA, distribution Eurimage.

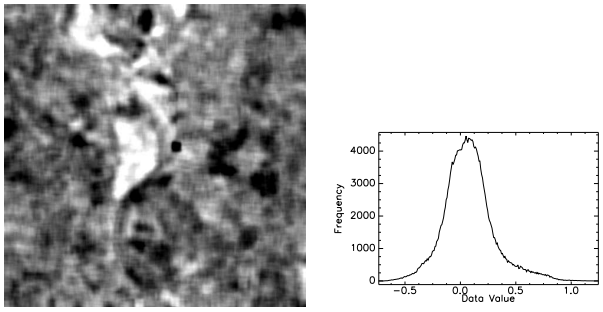

Fig. 10. Log-ratio image ($w = 15$) obtained from Fig. 9 and corresponding histogram.

To highlight the interest of the proposed approach, Fig. 11 presents the result obtained with f-HMC model under Gaussian densities assumption for $F = 3$ ($w = 15$). As detailed previously, the segmentation result produced by f-HMC model is not a binary one ("Change" / "NoChange" - black/white), but a fuzzy one (grey levels). Pixels intensities are proportional to the attributed fuzzy membership degrees. Bright intensities thus represent high proportion of "NoChange", and dark ones represent high proportion of "Change". The fuzzy HMC model is thus visually interesting on its own, since it allows an expert to interpret the change detection map with its proper knowledge.

As an indication, the f-HMC defuzzification result, presented in Fig. 12-(b), is obtained by performing a threshold at $\varepsilon = 0.5$ on the fuzzy classification result ($F = 3$). The corresponding HMC result (3-class) is presented in Fig. 12-(a). For both models, Gaussian densities were assumed. Indeed, one can easily distinguish in Fig. 12-(b) the main areas corresponding to the flood. Furthermore, HMC model seems to produce lots of false alarms in comparison to f-HMC one, which confirms results in Sec. V.

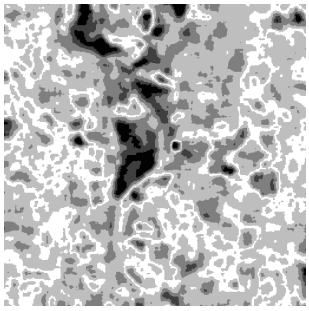

Fig. 11. Change detection maps obtained with f-HMC model with Gaussian distributions for $F = 3$ ($w = 15$).

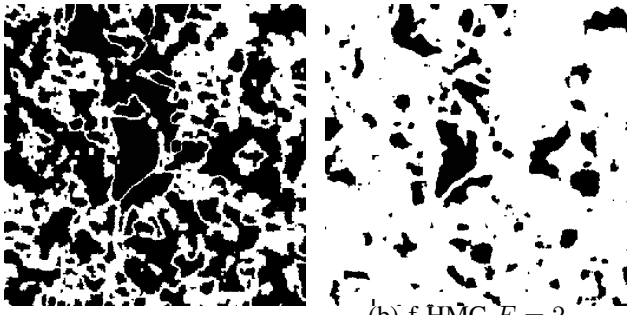

(a) HMC - $w = 15$. (b) f-HMC $F = 2$ - $w = 15$.

Fig. 12. Change detection maps obtained with HMC and f-HMC models with Gaussian distributions.

VII. Conclusion

In this work, we described a new fuzzy HMC model, with application to unsupervised fuzzy change detection on SAR images. The main contribution of this work is to combine both statistical and fuzzy approaches to address the unsupervised change detection task in the SAR context.

Experiments on bi-date sets of simulated images confirm the effectiveness of the proposed approach. Quantitative results show that the changed and unchanged distributions in log-ratio images can be modeled by Gaussian densities. Experiments conducted on real ERS-PRI bi-date images also confirm the interest of the model. Even if the f-HMC model seems not to be completely satisfying within an operational framework, the change map obtained with f-HMC appears to be in adequation with the feature image.

From this work, we plan to perform change detection in multi-temporal context by applying change vector analysis to the considered data set as follows: (1) compute a log-ratio vector by ratioing the different acquisitions pair by pair; (2) apply the vectorial f-HMC model [37] to the resulting multi-component data set in order to obtain the desired change detection map. Indeed, this approach will be clearly well-suited to the detection of long-term changes such as vegetation growth, desertification, ...

Last, the model is not restricted to the triangular-shaped membership function presented here, and any other membership functions (like trapezoidal- or Gaussian-shaped ones) can be used. The use of different membership functions allow to modify the characterization of the fuzzy classes, which constitutes an interesting perspective.

Acknowledgment

The authors are grateful to J. Inglada from the French Space Agency (CNES) for providing the co-registered SAR images. The authors are also grateful to G. Mercier from the GET/ENST Bretagne for valuable discussions on SAR image processing and change detection application.

References

[1] P. R. Coppin, I. Jonckheere, and K. Nachaerts, "Digital change detection in ecosystem monitoring: a review," *Int. J. of Remote Sensing*, vol. 24, pp. 1–33, 2003.

[2] D. Lu, P. Mausel, E. Brondizio, and E. Moran, "Change detection techniques," *Int. J. of Remote Sensing*, vol. 25, no. 12, pp. 2365–2407, 2004.

[3] E. Stabel and P. Fischer, "Detection of structural changes in river dynamics by radar-based earth observation methods," in *Proc. of the 1st Biennial Meeting of the Int. Environmental Modelling and Software Society*, vol. 1, Lugano, Switzerland, 2002, pp. 352–358.

[4] L. Bruzzone and D. F. Prieto, "An adaptive semiparametric and context-based approach to unsupervised change detection in multitemporal remote-sensing images," *IEEE Trans. Image Processing*, vol. 11, no. 4, pp. 452–466, April 2002.

[5] V. P. Onana, E. Trouvé, G. Mauris, J. P. Rudant, and P. L. Frison, "Change detection in urban context with multitemporal ERS-SAR images by using data fusion approach," in *IEEE Int. Conf. Geosci. Remote Sensing*, Toulouse, France, July 2003.

[6] J. Inglada, "Change detection on SAR images by using a parametric estimation of the kullback-leibler divergence," in *IEEE Int. Conf. Geosci. Remote Sensing*, Toulouse, France, July 2003.

[7] S. Derrode, G. Mercier, and W. Pieczynski, "Unsupervised change detection in SAR images using a multicomponent hidden Markov chain model," in *Analysis of Multi-temporal Remote Sensing Images*, ser. Remote Sensing, P. Smits and L. Bruzzone, Eds. Singapore: World Scientific, 2003, vol. 3, pp. 195–203.

[8] J. F. Mas, "Monitoring land-cover changes: a comparison of change detection techniques," *Int. J. of Remote Sensing*, vol. 20, no. 1, pp. 139–152, 1999.

[9] J. Inglada, "Similarity measures for multisensor remote sensing images," in *IEEE Int. Conf. Geosci. Remote Sensing*, vol. 1, Toronto, Canada, June 24-28 2002, pp. 104–106.

[10] P. Deer, "Digital change detection in remotely sensed imagery using fuzzy set theory," PhD Thesis, University of Adelaïde, Australia, Department of Geography and Computer Science, 1998.

[11] A. Singh, "Digital change detection techniques using remotely sensed data." *Int. J. of Remote Sensing*, vol. 10, no. 6, pp. 989–1003, 1989.

[12] S. Hegde, "Modelling land cover change: a fuzzy approach," Degree of master of science in geoinformatics, Int. Institute for Geo-Information Science and Earth Observation, Enschede, The Netherlands, December 2003.

[13] H. Nemmour and Y. Chibani, "Combining comparative and simultaneous analysis approaches based on fuzzy integration for change detection," in *XXth ISPRS Congress, Geo-Imagery Bridging Continents*, Istanbul, Turkey, July 12-23 2004, p. 709.

[14] K. B. Hilger and A. A. Nielsen, "Targeting input data for change detection studies by suppression of undesired spectra," in *of the Seminar on Remote Sensing and Image Analysis Techniques for Revision of Topographic Databases*. Copenhagen, Denmark: KMS, The National Survey and Cadastre, February 29 2000.

[15] P. Deer and P. Eklund, "Values for the fuzzy C-means classifier in change detection for remote sensing," in *Int. Conf. on Information Processing and Management of Uncertainty*, 2002, pp. 187–194.

[16] P. Agouris, S. Gyftakis, and A. Stefanidis, "Uncertainty in image-based change detection," in *4th Int. Symp. on Spatial Accuracy*, Amsterdam, Netherlands, July 2000, pp. 1–8.

[17] K. Aas, L. Eikvil, and R. Huseby, "Applications of hidden Markov chains in image analysis," *Pat. Recog.*, vol. 32, no. 4, pp. 703–713, 1999.

[18] R. Fjørtoft, Y. Delignon, W. Pieczynski, M. Sigelle, and F. Tupin, "Unsupervised segmentation of radar images using hidden Markov chains and hidden Markov random fields," *IEEE Trans. Geosci. Remote Sensing*, vol. 41, no. 3, pp. 675–686, 2003.

[19] L. Bruzzone and D. F. Prieto, "An MRF approach to unsupervised change detection," in *IEEE Int. Conf. Image Processing*, vol. 1, Kobe, Japan, October 25-28 1999, pp. 143–147.

[20] T. Kasetkasem and P. K. Varshney, "An image change detection algorithm based on Markov random field models," *Can. J. of Remote Sensing*, vol. 40, no. 8, pp. 1815– 1823, August 2002.
[21] C. Carincotte, S. Derrode, G. Sicot, and J. M. Boucher, "Unsupervised image segmentation based on a new fuzzy hidden Markov chain model," in *IEEE Int. Conf. Acoust., Speech, Signal Processing*, Montreal, Canada, May 17-21 2004.
[22] W. Pieczynski, "Statistical image segmentation," *Mach. Graph. and Vis.*, vol. 1, pp. 261–268, 1992.
[23] R. Touzi, A. Lopes, and P. Bousquet, "A statistical and geometrical edge detector for SAR images," *IEEE Trans. Geosci. Remote Sensing*, vol. 26, no. 6, pp. 764–773, November 1988.
[24] Y. Bazi, L. Bruzzone, and F. Melgani, "An approach to unsupervised change detection in multitemporal SAR images based on the generalized Gaussian distribution," in *IEEE Int. Conf. Geosci. Remote Sensing*, vol. 2, Anchorage, Alaska, USA, September 20-24 2004, pp. 1402–1405.
[25] ——, "An unsupervised approach based on the generalized Gaussian model to automatic change detection in multitemporal SAR images," *IEEE Trans. Geosci. Remote Sensing*, vol. 43, no. 4, pp. 874–887, April 2005.
[26] J. T. Kent and K. V. Mardia, "Spatial classification using fuzzy membership models," *IEEE Trans. Pattern Anal. Machine Intell.*, vol. 10, no. 5, pp. 659–671, September 1988.
[27] K. E. Avrachenkov and E. Sanchez, "Fuzzy Markov chains," *Fuzzy Optimization and Decision Making*, vol. 1, no. 2, pp. 143–159, June 2002.
[28] M. A. Mohamed and P. Gader, "Generalized hidden Markov models-Part I: Theorical frameworks," *IEEE Trans. Fuzzy Syst.*, vol. 8, no. 1, pp. 67–81, Feb. 2000.
[29] H. Caillol, W. Pieczynski, and A. Hillion, "Estimation of fuzzy Gaussian mixture and unsupervised statistical image segmentation," *IEEE Trans. Image Processing*, vol. 6, no. 3, pp. 425–440, 1997.
[30] H. Caillol, A. Hillion, and W. Pieczynski, "Fuzzy random fields and unsupervised image segmentation," *IEEE Trans. Geosci. Remote Sensing*, vol. 31, no. 4, pp. 801–810, July 1993.
[31] F. Salzenstein and W. Pieczynski, "Parameter estimation in hidden fuzzy Markov random fields and image segmentation," *Graph. Mod. and Im. Proc.*, vol. 59, no. 4, pp. 205–220, July 1997.
[32] S. Ruan, B. Moretti, J. Fadili, and D. Bloyet, "Fuzzy Markovian segmentation in application of magnetic resonance images," *Comp. Vis. and Im. Under.*, vol. 85, pp. 54–69, 2002.
[33] W. Skarbek, "Generalized Hilbert scan in image printing," in *Theoretical Foundations of Computer Vision*, R. Klette and W. G. Kropetsh, Eds. Berlin: Akademik Verlag, 1992.
[34] R. Dafner, D. Cohen-Or, and Y. Matias, "Context-based space filling curves," *Computer Graphics Forum*, vol. 19, no. 3, 2000.
[35] J. Hungershöfer and J. Wierum, "On the quality of partitions based on space-filling curves," in *Int. Conf. on Computational Science*, Amsterdam, The Netherlands, April 21-24 2002, pp. 36–45.
[36] N. Giordana and W. Pieczynski, "Estimation of generalized multisensor hidden Markov chains and unsupervised image segmentation," *IEEE Trans. Pattern Anal. Machine Intell.*, vol. 19, no. 5, pp. 465–475, 1997.
[37] C. Carincotte, S. Derrode, and S. Bourennane, "Multivariate fuzzy hidden Markov chains model applied to unsupervised multiscale SAR image segmentation," in *IEEE Int. Conf. Fuzzy Syst.*, Reno, Nevada, May 22-25 2005.

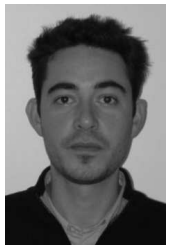

Cyril Carincotte received the image processing master from Aix-Marseille III University in June 2002, and the electronics and informatics engineering master from ISEN Lille in September 2002. Since October 2002, he works as PhD student in the multidimensional signal processing group (GSM), Fresnel Institute (CNRS UMR-6133), Marseille, France. His research interests include fuzzy hidden Markov models, applied to image segmentation and change detection issue.

Stéphane Derrode received the telecommunication engineering degree from Télécom Lille I, France in 1995, and the Ph.D. degree from the University of Rennes, France, in 1999. Since 2001, he has been with the École Généraliste d'Ingénieurs de Marseille, France, where he is currently an Associate Professor in the multidimensional signal processing group, Fresnel Institute (CNRS UMR-6133). His research interests include pattern recognition, image indexing and segmentation.

Salah Bourennane received his PhD degree from Institut National Polytechnique de Grenoble, France, in 1990 in signal processing. Currently, he is full Professor at the École Généraliste d'Ingénieurs de Marseille, France. His research interests include statistical signal processing, array processing, image processing, multidimensional signal processing and performances analysis.